RSC Advances

A gel single ion polymer electrolyte membrane for lithium-ion batteries with wide-temperature range operability

Yunfeng Zhang,[a,b] Rupesh Rohan[a], Yubao Sun*[b], Weiwei Cai,[a] Guodong Xu,[a] An Lin[c] and Hansong Cheng*[a,b]

[a]Department of Chemistry, National University of Singapore, 3 Science Drive 3, Singapore 117543

[b]Sustainable Energy Laboratory, China University of Geosciences Wuhan, 388 Lumo RD, Wuhan 430074, China

[c]College of Resource and Environmental Science, Wuhan University, Wuhan 430072, China

E-mail: chmch@nus.edu.sg

Abstract

We report excellent operability of a lithium-ion battery with a gel membrane of sp^3 boron-based single ion polymer, lithium poly (1,2,3,4-butanetetracarboxylic acid borate) (LiPBAB), as the electrolyte. The battery exhibits outstanding performance in a wide temperature range of 25 °C-100 °C with high ionic conductivity of 2.9×10^{-4} S cm^{-1}, high electrochemical stability of 4.3 V, a large cationic transference number t^+ of 0.89 and an excellent mechanical strength of 33 MPa at room temperature. The remarkable cyclic stability of the battery at 100 °C demonstrates exceptional device safety enabled by the electrolyte membrane.

Keywords: lithium ion battery, single ion polymer electrolyte, sp^3 boron, ionic conductivity, high temperature operation.

1. Introduction

As one of the most important secondary power sources for hybrid electric vehicles (HEVs) and plug-in electric vehicles (PEVs) and a storage medium for wind, solar and tidal energies in smart grids, lithium ion batteries have been in increasingly high demand for continuous technological advancement.[1-7] While electrodes regulate the

1

energy capacity of the batteries, electrolyte, which works as a mediator to facilitate lithium-ion shuttling between the electrodes, plays a vital role in modulating the overall battery performance.[8] Typical commercial electrolytes are prepared by dissolving lithium salts in selected organic solvents such as propylene carbonate (PC) and ethylene carbonate (EC).[7-9] These electrolytes offer high ionic conductivity on the order of 10^{-3} S cm^{-1} in these solvents. However, the high flammability and the inherent concentration polarization upon charging/discharging associated with the lithium salts dissolved in the organic solvents have raised serious concerns on the battery safety and performance. [10-12]

Solid polymer electrolytes provide a promising alternative to enhance battery safety.[13-16] Unfortunately, the low ionic conductivity ranging from 10^{-8} to 10^{-5} S cm^{-1} at near ambient temperatures and the poor mechanical strength have been the main obstacles that have hindered broad applications of the battery devices.[18] To overcome this problem, a concept of gel polymer electrolyte (GPE) by dispersing a small molecular electrolyte salt in a low temperature flexible polymer matrix was proposed as a compromise between liquid electrolytes and solid polymer electrolytes.[19] With an ionic conductivity up to 10^{-3} S/cm at room temperature, the liquid organic adsorbed GPEs is capable of providing an enhanced safety operation and compatibility with the electrodes in the charge-discharge cycling processes.[20] Nevertheless, formation of a strong lithium salt concentration gradient in battery operation, arising from the low lithium ion transference number of small molecular lithium salts (<0.3), leads to dendrite growth and ultimately limits power delivery.[21] Significant efforts have been made to enhance the lithium ion transference number by adding fillers into a polymer matrix as a solid plasticizer.[22-24] For example, Croce and his co-workers[25] added a sulphate-promoted superacid zirconia (ZrO$_2$) into a poly(ethylene oxide)-lithium tetrafiuoroborate matrix to achieve an improved lithium ion transference number of 0.42 ± 0.05, still much lower than the unity.

An effective solution to the problem is conceived by developing single ion conductive polymer electrolytes (SIPEs) with partially delocalized anions on polymer backbones

and lithium ions attached to the polymers via a weak electrostatic interaction.[27-30] It has been demonstrated in several recent reports that SIPEs offer extensive advantages over the conventional liquid electrolytes and GPEs with a wide electrochemical window, good thermal stability and high conductivity ($> 10^{-4}$ S/cm at room temperature) in addition to a high lithium transference number close to unity.[26, 31-32] Several recent studies have demonstrated highly promising battery performance with SIPE membranes.[31-33] However, only a few SIPE equipped Li-ion batteries were found to exhibit wide temperature range operability.[26] In particular, to date, there has been no report on SIPE-based Li-ion batteries that exhibit a wide temperature range activity at both room temperature and high temperature up to $100\ ^{\circ}$C simultaneously.

One class of SIPE materials is based on incorporation of a sp^3 boron configuration into the polymeric structures. The boron atoms are covalently bonded with electron withdrawing groups in these compounds, resulting in charge delocalization in the polymer chains. The boron incorporation naturally leads to induction of lithium ions in the interstitials with a weak electrostatic interaction with the anions covalently bonded to the polymers, which thus gives rise to high lithium ion mobility and high conductivity. The concept of using sp^3 boron in electrolytes as a counter ion of lithium ions is not new. In fact, the idea was utilized to develop a highly successful small molecular lithium salt, LiBOB, a decade ago.[34-35] However, only recently, the polymeric analogues of LiBOB have been reported.[36-38] The sp^3 boron-based polymeric materials do not suffer from the concentration polarization commonly observed in liquid electrolytes of small inorganic lithium salts and their membranes can be readily fabricated via solution cast processes. In a recent communication, we reported successful synthesis of several sp^3 boron based SIPE compounds.[39] The fabricated SIPE membranes by using a special solvent-thermal method display high lithium ion conductivity on the order of 10^{-3} S cm^{-1} with excellent thermal stability and a wide electrochemical window. Unfortunately, the poor mechanical strength and uncontrolled high thickness of the fabricated SIPE membranes result in no battery activity even at an elevated temperature.

In this paper, we report significantly improved performance of one of the SIPE membranes comprised of a blend of lithium poly (1,2,3,4-butanetetracarboxylic acid borate) (LiPBAB) and PVDF-HFP fabricated by a solution cast method. With tuneable thickness and flexibility, the membrane displays excellent mechanical strength and high ionic conductivity. The assembled lithium battery exhibits remarkable electrochemical performance in the operating temperature range from 25 ^{o}C to 100 ^{o}C, demonstrating the excellent safety and broad applicability of the battery device.

2. Experimental

2.1. Materials

1,2,3,4-butanetetracarboxylic acid (99.99%) (Sigma Aldrich), hexamethyldisilazane (Sigma Aldrich), dichloroethane (DCE) (Sigma Aldrich), trimethylborate (Sigma Aldrich), PVdF-HFP (Sigma Aldrich), acetylene black (Sigma Aldrich), LiFePO$_4$ (Sigma Aldrich), acetonitrile (Fisher). DCE and acetonitrile were dried over phosphorus (V) oxide, while methanol was dried over magnesium/iodine prior to use.

2.2. Synthesis of lithium poly (1,2,3,4-butanetetracarboxylic acid borate) (LiPBAB)
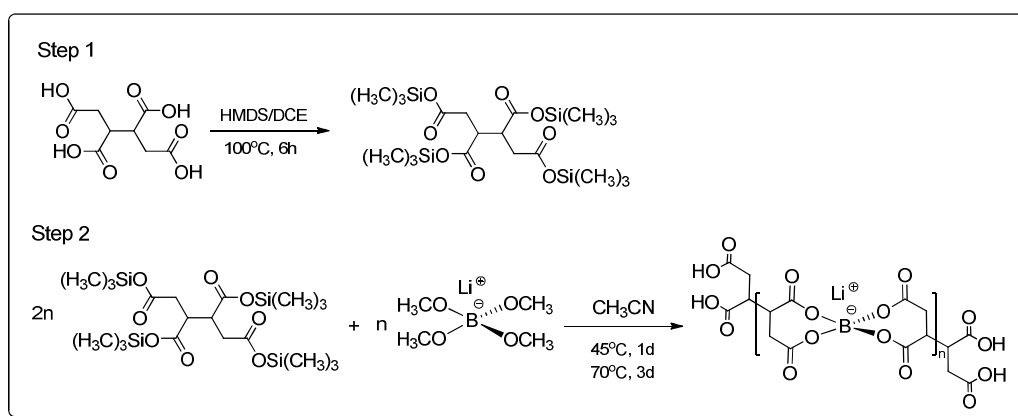
Scheme 1. The synthetic procedure of LiPBAB.

The synthesis of LiPBAB was performed in two steps. In the first step, a silylation reaction was carried out under argon atmosphere by reacting 4.6832 g of 1,2,3,4-butanetetracarboxylic acid (20 mmol) with 10 ml of hexamethyldisilane

(HMDS) (50 mmol) in anhydrous DCE at 100 °C till all acidic moieties were consumed (ca. 6 hrs). The white solid product was precipitated out after the DCE and unreacted HMDS were removed under a reduced pressure. ^{1}H NMR (DMSO-d6): δ 3.80 (2H, d), δ 3.12 (2H, d), δ0.20 (18H, s) (Fig. 1).
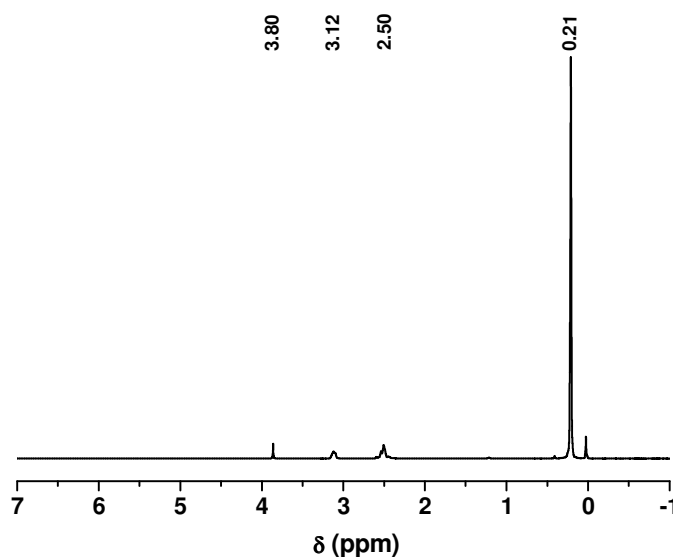

Figure 1. The ^{1}H NMR spectrum of silylation derivative of 1,2,3,4-butanetetracarboxylic acid.

In the second step, the reaction was done by stirring lithium tetramethanolatoborate and the silylation derivative of 1,2,3,4-butanetetracarboxylic acid (product of step 1) in an anhydrous acetonitrile (ACN) at 45 °C for 1 day and subsequently at 70 °C for another 3 days. The raw product was purified via washing with ACN. After drying at 120 °C under vacuum for 24 hrs, the final product (LiPBAB) was collected and stored in the argon-filled glove box for further characterizations.

2.3. Preparation of single ion conductor membrane

The PVdF-HFP/LiPBAB membrane was prepared via a solution cast method.[40] 0.15 g of PVdF-HFP and 0.05g of LiPBAB were dissolved in a 8 ml of DMF solvent at 80 °C to form a homogeneous solution. The solution was subsequently casted onto a glass petri dish and kept in an oven at 80 °C for 24 hrs to evaporate DMF. A trace amount of DMF was fully removed under vacuum at 80 °C for two days. Finally, the

membrane was transferred to an argon-filled glove box and stored in a mixture of EC/PC (v:v, 1:1) solvents for further characterizations.

Electrochemically, the thickness of a membrane may exert a strong influence on battery performance. In general, a thinner membrane offers a lower resistance, which leads to better battery performance; however, it may also give rise to serious issues on mechanical strength, making the battery fragile for short-circuiting. Therefore, a delicate balance between mechanical strength and resistivity must be considered for membrane fabrication. It was reported that a thickness of 50-100 μm is adequate to achieve sufficient mechanical strength.[26, 31, 32] In the present study, we chose 50 μm for the membrane after considering both electrochemical performance and mechanical properties.

2.4. Methods

Molecular weight and poly dispersity index (PDI) were measured by Gel Permeation Chromatography (GPC) (Waters 515 HPLC Pump, Waters 2707 Autosampler, Waters 2414 Refractive Index Detector). Pure water was used as an eluent at a flow rate of 0.8 ml min^{-1}. The polyethylene oxide (PEO) standard was used for calibration. All infrared spectra were taken with a Bio-Rad Excalibur FTIR spectrometer in the 400-4000 cm^{-1} frequency range. ^{1}H and ^{11}B NMR spectra were recorded on a Bruker AMX (500) spectrometer at 500 MHz with trifloroborane (BF$_3$) in ether solution (as the standard). Dimethyl sulfoxide-d6 and deuterium oxide were used as solvents for NMR test. Powder X-Ray Diffraction (XRD) was performed on a D5005 Bruker AXS diffractometer with the sample size of 70-110 mg and Cu-Kα radiation ($\lambda = 1.5410$) as the source at 40 kV voltage in the scanning range between 1.4° and 60° at room temperature . The morphologies of the polymer electrolytes were probed using the Scanning Electron Microscopy (SEM) with QUANTA 200 FEG. Samples were prepared by platinum sputtering under 5×10^{-2} mbar at room temperature (20s, 30mA) with a Baltec SCD050 apparatus. The thermal degradation study was performed under inert atmosphere of N$_2$ (flow rate: 60 cm^3 min^{-1}) as well as in air, at the 10 $^{\circ}$C min^{-1}

heating rate in the Thermo Gravimetric Analyzer (model TGA Q 50) of TA, Inst., USA. The thermal stability test was conducted from room temperature to 800 $^{\circ}$C.

The ion conductivity of the polymer electrolytes was measured by Electrochemical Impedance Spectroscopy (EIS) using the Zahner potentiostate-galvanostatate electrochemical workstation model, PGSTAT, with the EIS module over a frequency range of 4×10^6 to 1 Hz and an oscillating voltage of 5 mV. A stainless steel cylindrical device of 1.5 cm diameter was used for conductivity measurement. The fitting of the raw data was done by using the Simulated Impedance Measurement (SIM) software. The electrochemical stability test (cyclic voltammetry) was conducted in the same stainless steel device using the CHi instrument in the voltage range of 1.5-7 volts at a scan rate of 2 mV S^{-1}. A circular thin sheet of lithium metal along with the electrolyte membrane was placed inside the cavity of the device and sealed in a glove box under argon atmosphere. The lithium-ion transference number, t^+, was measured for the Li/SIPE membrane/Li battery cell, in which the electrolyte membrane soaked in a EC/PC solution was mounted between the two non-blocking lithium metal electrodes.[16, 41] The value of t^+ was measured by the combination of complex impedance and potentiostatic polarization methods proposed by Evans et al.,[42] and was then calculated using the following equation:

$$t^+ = \frac{I_s(\Delta V - I_0 R_0)}{I_0(\Delta V - I_s R_s)}$$

where ΔV is the potential applied across the cell, I_0 and I_s are the initial and steady-state currents and R_0 and R_s are the initial and steady-state resistances of the passivation layers on the Li electrode.

To analyse the battery performance, a multichannel battery testing instrument Arbin BT-2000 was used for the discharge capacity measurement of the coin cells assembled with the synthesized polymeric electrolyte membrane. The composite cathode was prepared by casting a well stirred solution of $LiFePO_4$ (75 wt.%), PVdF (10 wt.%), acetylene black (10 wt.%) and a small amount of lithium bis(4-carboxy phenyl sulfonyl)imide (5 wt.%) as a supporting electrolyte in a NMP solvent on to an

7

aluminum foil. The resulting electrode was initially dried at 60 ^{o}C and further dried at 60 ^{o}C in a vacuum oven for 12 hours. The dried cathode was then cut into a circular shape used in coin cells. The assembling of the standard coin cells (CR2025) was done inside a glove box.

3. Results and Discussion

3.1. Synthesis

Successful synthesis of the proposed structure of LiPBAB is verified by the ^{1}H NMR, ^{13}C NMR, ^{11}B NMR, FTIR and GPC characterizations. The ^{1}H NMR (D$_2$O) peaks at 2.80 (2H, m), δ 2.50 (2H, m), δ 2.38 (2H, m) (Figure 2a) and the ^{13}C NMR (D$_2$O) peaks at 179.19 (s, CH$_2$COO), 177.89 (s, CHCOO), 46.31 (s, CH), 36.95 (s, CH$_2$) (Figure 2b) agree well with of the corresponding signals of the 1,2,3,4-butanetetracarboxylic acid precursor. The ^{11}B NMR spectrum (Figure 2c) exhibits a peak at 0.66 ppm, reflecting a typical *sp^3* hybridized state of boron atoms.[43] The FT-IR peaks at 1310, 1252, 1221 and 1013 cm^{-1} correspond to the stretch of the B-O bond stretching   while   the peaks at 1674 and 1693 cm^{-1} correspond the C=O bonds of the carboxylic group.[44-45] The number-average molecular weight (M_n), the weight average molecular weight (*Mw*) and poly dispersity index (PDI) of LiPBAB, obtained from GPC analysis, are 29,400, 32,000 and 1.16, respectively, validating a polymeric structure with a narrow distribution of the molecular weights.
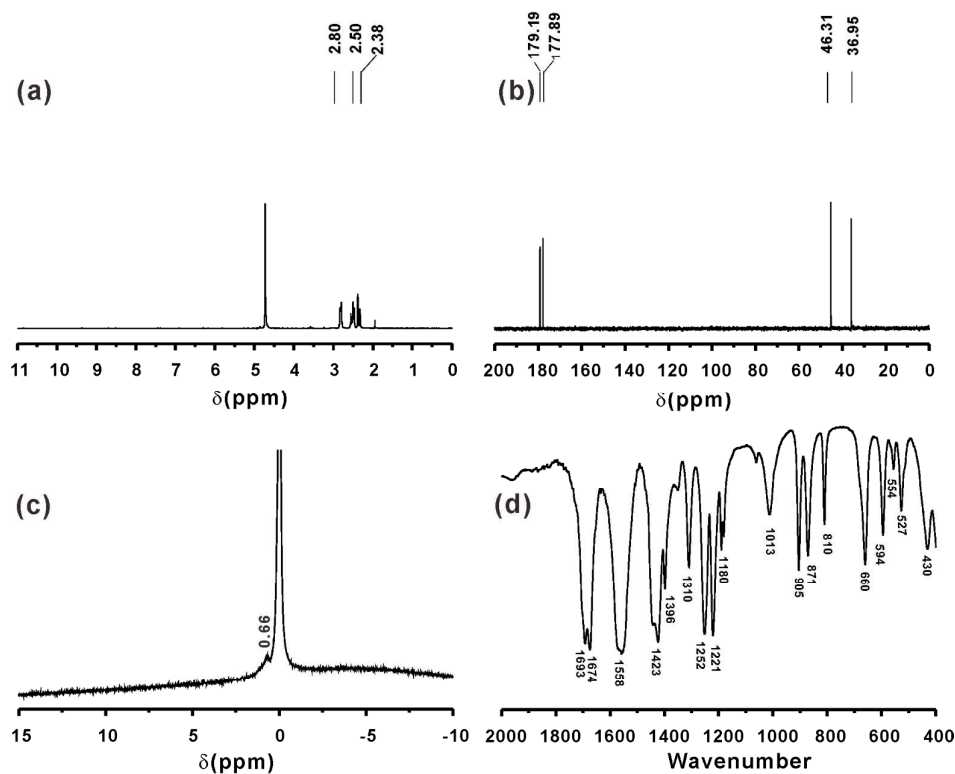
Figure 2. Characterizations of LiPBAB. (a) The ^{1}H NMR spectrum, (b) the ^{13}C NMR spectrum, (c) the ^{11}B NMR spectrum, and (d) the FT-IR spectrum.

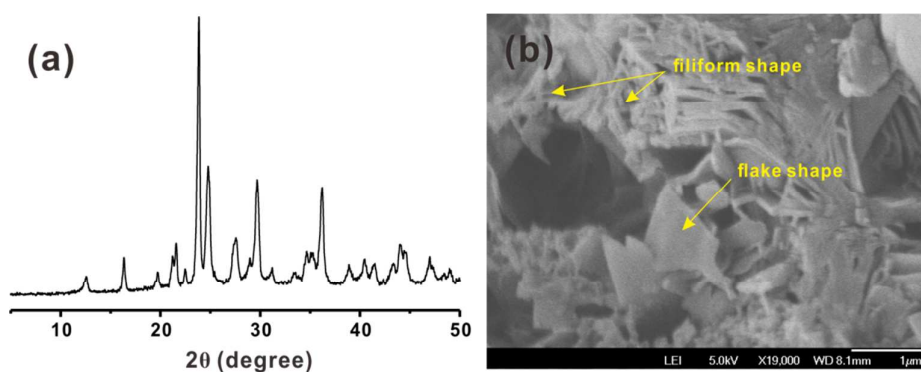### 3.2. Morphology and microstructure characterization

Figure 3. The SEM image and the XRD spectrum of LiPBAB.

The XRD pattern of LiPBAB (Figure 3a) displays sharp diffraction peaks, suggesting good crystallinity with a long range order, well corroborated by the filiform shapes shown in the SEM image (Figure 3b). The existence of the flake shape structures

suggests that a planar structure of LiPBAB may also be formed, similar to the previous reported work.[39]
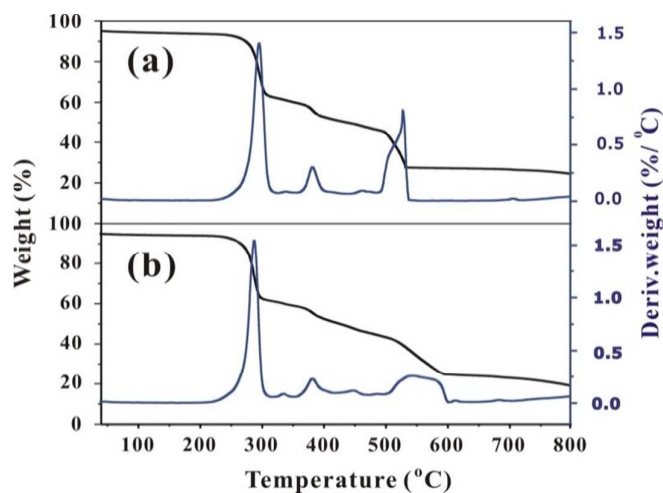
3.3. Thermal properties

Figure 4. The thermal and thermo-oxidative stabilities of LiPBAB under: (a) nitrogen atmosphere and (b) oxygen atmosphere.

The thermal degradation curves of LiPBAB under both nitrogen atmosphere and air display a three stage decomposition trend starting at 245 ^{o}C. The results reveal excellent thermal stability of the compound and confirm the material suitability for Li-ion batteries for safe operation at elevated temperatures.

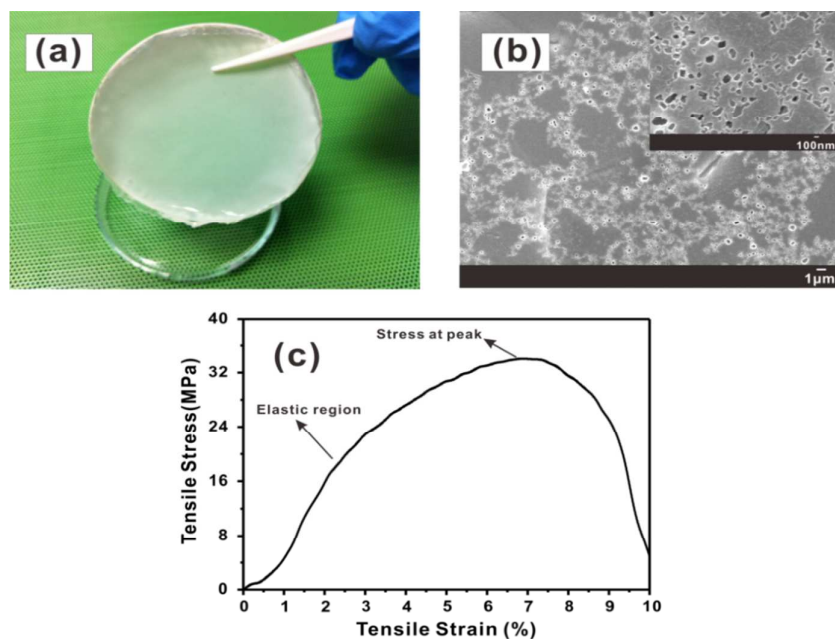*3.4. Surface morphology of single ion conducting membranes*

Figure 5. The photograph (a), surface morphology (b), and mechanical strength of the PVdF-HFP/LiPBAB membrane.

A smooth electrolyte membrane with adequate mechanical strength can effectively prevent lithium dendrite formation.[46] The morphology and the tensile stress/strain graph of PVdF-HFP/LiPBAB membrane are shown in Figure 5. Figures 5a and 5b illustrate excellent uniformity of the membrane surface at both macro and micro levels. From the stress-strain curve of the membrane shown in Figure 5c, the tensile strength was derived to be 33 MPa, higher than the reported value in a similar study.[31] Hence, the robustness and the uniformity of the membrane make the film more resistant against lithium dendrite formation.

Appropriate porosity of an electrolyte membrane is an essential requirement for facile transport of Li-ions.[47-48] It has been well demonstrated that a pore size of less than 1 µm is most beneficial for Li batteries to avoid both lithium dendrite formation and solvent leakage.[50-53] The SEM image of the LiPBAB membrane displayed in Figure 5b shows a porous structure with an average pore diameter of 100 nm, which falls into the range of the recommended size. The high porosity of the PVdF-HFP/LiPBAB membrane is confirmed by the large solvent uptake of 126 wt. %, making this

material well suited for serving as an electrolyte membrane. We note here that the downside of the high solvent retention in the electrolyte membranes is that batteries equipped with the membranes would not be as safe as those with all solid electrolytes although gel electrolytes in general possess higher ionic conductivity and better interfacial resistance.
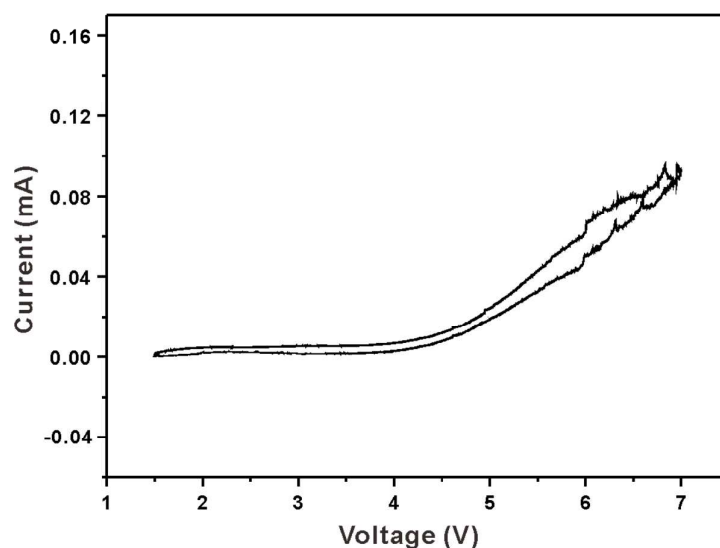
3.5. Electrochemical stability

Figure 6. The electrochemical stability window of the PVdF-HFP/LiPBAB membrane.

The electrochemical stability of LiPBAB was studied via cyclic voltammetry measurement using a Li/GPE/stainless steel cell for the EC/PC swollen PVdF-HFP/LiPBAB membrane (Figure 6). In the potential range of 2.5 - 4.3 V (vs Li/Li$^+$), no significant increase in the oxidation current is observed. The results clearly indicate that the LiPBAB electrolyte membrane is electrochemically stable.

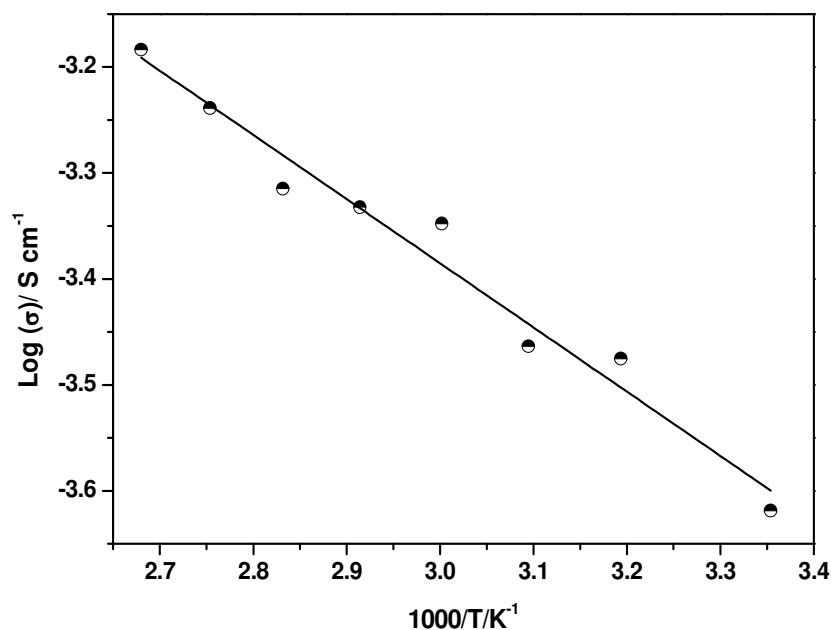*3.6. Ionic Conductivity and lithium ion transference number*

Figure 7. The ionic conductivity of the PVdF-HFP/LiPBAB membrane vs. the inverse of temperature.

Figure 7 depicts the temperature dependence of the ionic conductivity of the PVdF-HFP/LiPBAB membrane. The variation of the ionic conductivity displays a typical behaviour of an Arrhenius graph over the temperature range from $100\,^{\circ}$C to 20 $^{\circ}$C downwards. The ionic conductivity at 20 $^{\circ}$C was found to be 2.4×10^{-4} S/cm. Indeed, the measured conductivity increases with temperature but not completely linear, which may be attributed to the mechanical coupling between ion transport and polymer host mobility at a given temperature according to the free volume law.[54-55] The highest measured conductivity of the membrane at $100\,^{\circ}$C is 6.9×10^{-4} S cm^{-1}.
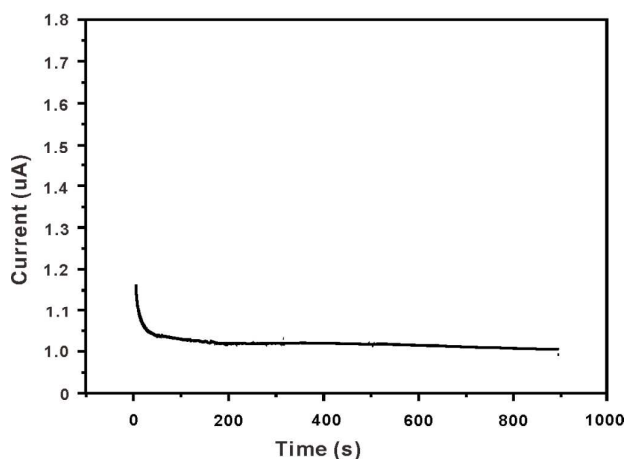
Figure 8. The time-dependent response of dc polarization for the Li|PVDF-HFP/LiPBAB|Li symmetric cell polarized with a potential of 100 mV.

The lithium transference number, t^+, measured by the method proposed by Evans et al.,[42] was found to be 0.87 at room temperature (Figure 8 and Table 1), much higher than that of LiBOB based electrolytes (< 0.60)[56] and the trilayer PVdF/polyborate/PVdF gel polymer electrolyte doped with $LiPF_6$ (0.58).[32] The significantly higher value of t^+ of the LiPBAB membrane confirms that the polymer electrolyte indeed exhibits a single-ion behavior, as expected, due to the restricted movement of anions as the part of polymer backbones, in contrast to the dual-ion conductors such as LiBOB.[31]

Table 1. The measured initial and steady-state currents, the initial and steady-state resistances of the passivation layers on the Li electrode and the ion transference number.

Electrolytes	$I_0(\mu A)$	$I_s(\mu A)$	$R_0(\Omega)$	$R_s(\Omega)$	$t^+=\frac{I_s(\Delta V-I_0R_0)}{I_0(\Delta V-I_sR_s)}$
LiPBAB	1.16	1.02	12.60	12.80	0.87

3.7. Battery performance

To examine the performance of the PVdF-HFP/LiPBAB membrane in Li-ion batteries, several coin cells were assembled with the membrane, using $LiFePO_4$ as the cathode and a lithium foil as the anode. Figure 9 displays the discharge capacity vs. the cycle number of the Li|PVdF-HFP(EC/PC)/LiPBAB|LiFePO$_4$ cell at different

14

charge/discharge rate at   three different temperatures. Unlike most of the SIPE equipped batteries, these batteries do show an appreciable room temperature performance with the discharge capacity of 135 mAhg^{-1} at C/10 rate, which infers facile lithium ion transportation via this membrane, even at room temperature.[32,26, 31] The performance improves at the operating temperature of 80 $^{\circ}$C as discharge capacity touches the mark of 150 mAhg^{-1} at C/10 rate, and it could also perform at the high rate of C/2 with the discharge capacity of 110 mAhg^{-1} at the same temperature. More remarkably, even at 100 $^{\circ}$C, the battery is still fully operational and maintains the discharge capacity of 110 mAhg^{-1} at 1 C. Resetting the C-rate to C/10 still results in the high discharge capacity of 151 mAhg^{-1} after 170 cycle performance test at various C-rates and temperatures, indicating that the SIPE-based battery is highly robust with superior thermal, mechanical and electrochemical stability

The excellent high temperature performance of the SIPE-based battery indicates that the organic solvent used in the polymer membrane to enhance ionic conductivity and to reduce the interfacial resistance between the membrane and electrodes would not present a potential safety hazard as in the case of batteries with liquid electrolytes and gel-polymer electrolytes. We speculate that the reason for the superior stability in the SIPE-based batteries at high temperatures lies in the low concentration polarization in the electrolyte membranes that effectively prevent the organic solvents from decomposition in the electrochemical process.
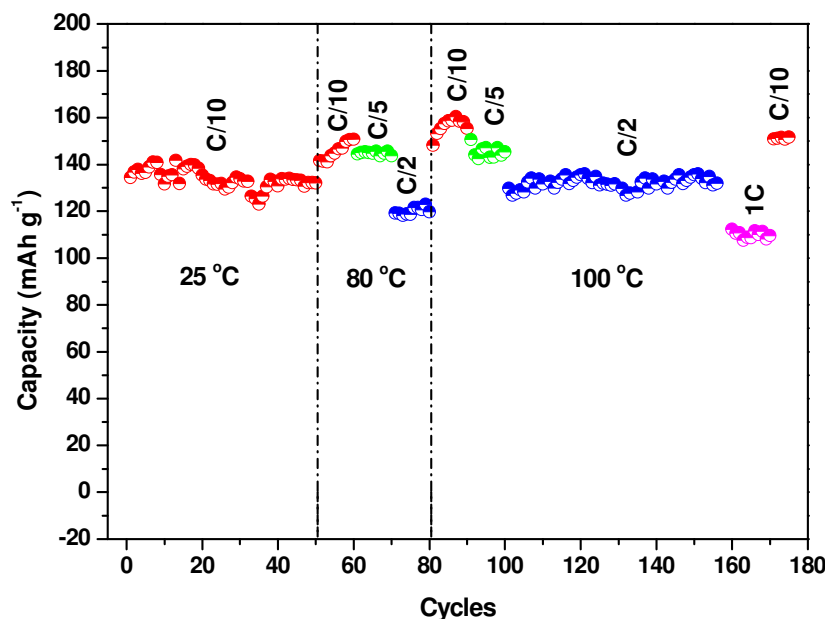
Figure 9. The cycling performance of the Li/PVdF-HFP/LiPBAB|LiFePO$_4$ battery in the temperature range of 25 ^{o}C to 100 ^{o}C and C/n rates.

4. Summary

We have presented a two-step process to synthesize a *sp^3* boron-based single ion conducting polymer electrolyte (LiPBAB) through copolymerization between lithium tetramethanolatoborate (LiB(OCH$_3$)$_4$) and a silylated 1,2,3,4-butanetetracarboxylic acid precursor. A thin, flexible and mechanically robust SIPE membrane was fabricated by blending LiPBAB with PVDF-HFP through a solution cast method. With the cationic transference number of 0.87, the membrane shows electrochemical stability up to 4.3 V and thermal stability up to 245 ^{o}C. The membrane is mechanically stable with the tensile strength of 33 MPa. The ionic conductivity of the membrane was found to be on the order of 10^{-4} to 10^{-3} Scm^{-1} in the temperature range from room temperature to 100 ^{o}C, which is comparable to the conductivity of liquid electrolytes of small inorganic lithium salts.

The performance of the SIPE membranes in Li-ion batteries was analysed by constructing Li|PVDF-HFP/LiPBAB|LiFePO$_4$ half cells followed by testing the batteries in the temperature range of 25 ^{o}C - 100 ^{o}C at various charge/discharge rates.

16

The batteries display remarkable performance at room temperature, unlike most of the reported SIPE-based Li-ion batteries which are operative only at an elevated temperature. The battery performance, in the context of both discharge capacity and high C-rates, is enhanced as temperature increases. Our results show that the use of organic solvent in the SIPE electrolyte membrane in the battery cell can significantly boost battery performance through enhancement of ionic conductivity. However, contrary to the conventional wisdom that even a gel polymer electrolyte would not be safe at elevated temperatures with organic solvents in the polymer matrix, the battery with the PVDF-HFP/LiPBAB electrolyte membrane containing a EC/PC solvent displayed excellent performance at a temperature as high as 100 $^{\circ}$C. The results demonstrate the outstanding safe operation of the batteries equipped with the LiPBAB membrane at a wide temperature range.

Acknowledgment

Reference

1 N. Kamaya, K. Homma, Y. Yamakawa, M. Hirayama, R. Kanno, M. Yonemura, T. Kamiyama, Y. Kato, S. Hama, K. Kawamoto and A. Mitsui, *Nat Mater.* 2011, **10**, 682-686.

2 B. Scrosati, *Electrochimica Acta.* 2000, **45**, 2461-2466.

3 A. Väyrynen and J. Salminen, *J Chem Thermodyn.*, 2012, **46**, 80-85.

4 F. Croce, A. D'Epifanio, J. Hassoun, P. Reale and B. Scrosati, *J. Power Sources,* 2003, **119-121**, 399-402.

5 B. Scrosati and R. Neat in *Lithium polymer batteries*, *Vol.* (Ed. B. Scrosati), Springer Netherlands, **1993**, pp. 182-222.

6 K. Xu, *Chem. Rev.*, 2004, **104**, 4303-4417.

7 B. Scrosati and J. Garche, *J. Power Sources,* 2010, **195**, 2419-2430.

8 K. Xu, *Chem. Rev.*, 2004, **104**, 4303-4418.

9 D. W. McOwen, D. M. Seo, O. Borodin, J. Vatamanu, P. D. Boyle and W. A. Henderson, *Energ Environ Sci.,* 2014.

10 J. B. Goodenough and K.-S. Park, *J Am Chem Soc.,* 2013, **135**, 1167–1176.

11 TASAKI, Ken, GOLDBERG, Alex, LIAN, Jian-Jie, WALKER, Merry, TIMMONS, Adam, HARRIS and S. J., Electrochemical Society, Pennington, NJ, ETATS-UNIS, **2009**, p.

12 L. J. Krause, W. Lamanna, J. Summerfield, M. Engle, G. Korba, R. Loch and R. Atanasoski, *J. Power Sources.* 1997, **68**, 320.

13 X. Zuo, X.-M. Liu, F. Cai, H. Yang, X.-D. Shen and G. Liu, *J Mater Chem.*, 2012, **22**, 22265-22271.

14 L. Jin, P. Howlett, J. Efthimiadis, M. Kar, D. Macfarlane and M. Forsyth, *J Mater Chem.*, 2011, **21**, 10171-10178.

15 Y. Lin, J. Li, Y. Lai, C. Yuan, Y. Cheng and J. Liu, *RSC Advances.* 2013, **3**, 10722-10730.

16 S. Feng, D. Shi, F. Liu, L. Zheng, J. Nie, W. Feng, X. Huang, M. Armand and Z. Zhou, *Electrochimica Acta.* 2013, **93**, 254-263.

17 W. X. Chen, Z. D. Xu and L. S. Yang, *J Power Sources*, 2001, **102**, 112-117.

18 E. Quartarone and P. Mustarelli, *Chem. Soc. Rev.*, 2011, **40**, 2525-2540.

19 J. M. Tarascon, A. S. Gozdz, C. Schmutz, F. Shokoohi and P. C. Warren, *Solid State Ion.*, 1996, **86-88, Part 1**, 49-54.

20 J. B. Goodenough and Y. Kim, *Chem Mater.*, 2009, **22**, 587-603.

21 D. R. MacFarlane, J. Huang and M. Forsyth, *Nature.* 1999, **402**, 792-794.

22 J. E. Weston and B. C. H. Steele, *Solid State Ionics.* 1982, **7**, 75-79.

23 C. Capiglia, P. Mustarelli, E. Quartarone, C. Tomasi and A. Magistris *Solid State Ion.*, 1999, **118**, 73-79.

24 F. Croce, G. B. Appetecchi, L. Persi and B. Scrosati, *Nature.* 1998, **394**, 456-458.

25 F. Croce, L. Settimi and B. Scrosati, *Electrochem. Commun.*, 2006, **8**, 364-368.

26 R. Bouchet, S. Maria, R. Meziane, A. Aboulaich, L. Lienafa, J.-P. Bonnet, T. N. T. Phan, D. Bertin, D. Gigmes, D. Devaux, R. Denoyel and M. Armand, *Nat Mater.* 2013, **12**, 452-457.

27 M. Watanabe, Y. Suzuki and A. Nishimoto, *Electrochimica Acta.* 2000, **45**, 1187-1192.

28   D. Benrabah, S. Sylla, F. Alloin, J. Y. Sanchez and M. Armand, *Electrochimica Acta.*
      1995, **40**, 2259-2264.

29   K. Onishi, M. Matsumoto, Y. Nakacho and K. Shigehara, *Chem Mater.*, 1996, **8**,
469-472.

30   Y. Tada, M. Sato, N. Takeno, Y. Nakacho and K. Shigehara, *Chem Mater.*, 1994, **6**,
27-30.

31   X. Wang, Z. Liu, C. Zhang, Q. Kong, J. Yao, P. Han, W. Jiang, H. Xu and G. Cui,
      Electrochimica Acta. 2013, **92**, 132-138.

32   Y. Zhu, S. Xiao, Y. Shi, Y. Yang and Y. Wu,   *J Mater Chem A*, 2013, **1**, 7790-7797.

33   R. Rohan, Y. Sun, W. Cai, K. Pareek, Y. Zhang, G. Xu and H. Cheng, *J Mater Chem A*,
      2014, **2**, 2960-2967.

34   W. Xu and C. A. Angell, *Electrochem. Solid-State Lett.,* 2001, **4**, E1-E4.

35   K. Xu, S. Zhang, T. R. Jow, W. Xu and C. A. Angell, *Electrochem. Solid-State Lett.,*
      2002, **5**, A26-A29.

36   X.-G. Sun, J. B. Kerr, C. L. Reeder, G. Liu and Y. Han, *Macromolecules.* 2004, **37**,
      5133-5135.

37   X.-G. Sun, C. L. Reeder and J. B. Kerr, *Macromolecules.* 2004, **37**, 2219-2227.

38   X.-G. Sun and J. B. Kerr, *Macromolecules.* 2005, **39**, 362-372.

39   Y. Zhang, G. Xu, Y. Sun, B. Han, T. B. W. T, Z. Chen, R. Rohan and H. Cheng, *RSC
      Adv.*, 2013, **3**, 14934-14937.

40   Y. Zhang, Y. Sun, G. Xu, W. Cai, R. Rohan, A. Lin and H. Cheng, *Energy Technology.*
      2014. DOI: 10.1002/ente.201402010

41   A. Ghosh, C. Wang and P. Kofinas, *J Electrochem Soc.,* 2010, **157**, A846-A849.

42   J. Evans, C. A. Vincent and P. G. Bruce, *Polymer.* 1987, **28**, 2324-2328.

43   I. M. Malkowsky, R. Fröhlich, U. Griesbach, H. Pütter and S. R. Waldvogel, *Eur J Inorg
      Chem.,* 2006, **2006**, 1690-1697.

44   L. Larush-Asraf, M. Biton, H. Teller, E. Zinigrad and D. Aurbach, *J Power Sources*,
      2007, **174**, 400-407.

45   A. O. Mona, M. A. Amr and A. E. Hatem, *Processing and Application of Ceramics.*
      2012, **6**, 141-149.

46   W. Yi, Z. Huaiyu, H. Jian, L. Yun and Z. Shushu, *J Power Sources*, 2009, **189**, 616-619.

47   T.-H. Cho, M. Tanaka, H. Onishi, Y. Kondo, T. Nakamura, H. Yamazaki, S. Tanase and
      T. Sakai, *J Power Sources*, 2008, **181**, 155-160.

48   Y. Liang, L. Ji, B. Guo, Z. Lin, Y. Yao, Y. Li, M. Alcoutlabi, Y. Qiu and X. Zhang, *J
      Power Sources*, 2011, **196**, 436-441.

49   L. Persi, F. Croce and B. Scrosati, *Electrochem. Commun.*, 2002, **4**, 92-95.

50   P. Arora and Z. Zhang, *Chem. Rev.*, 2004, **104**, 4419-4462.

51   M. Yang and J. Hou, *Membranes.* 2012, **2**, 367-383.

52   S. S. Zhang, *J Power Sources*, 2007, **164**, 351-364.

53   Q. Shi, M. Yu, X. Zhou, Y. Yan and C. Wan, *J Power Sources*, 2002, **103**, 286-292.

54   O. E. Geiculescu, J. Yang, S. Zhou, G. Shafer, Y. Xie, J. Albright, S. E. Creager, W. T.
      Pennington and D. D. DesMarteau, *J Electrochem Soc.,* **151**, A1363-A1368.

55   R. Meziane, J.-P. Bonnet, M. Courty, K. Djellab and M. Armand, *Electrochimica Acta.*
      2011, **57**, 14-19.

56   W. Xua, A. J. Shustermanb, M. Videac, V. Velikova, R. Marzked and C. A. Angell *J Electrochem Soc.,* 2003, **150**, E74-E80.